Hindawi Publishing Corporation
Journal of Nanomaterials
Volume 2013, Article ID 714853, 6 pages
http://dx.doi.org/10.1155/2013/714853

*Research Article*

# CuO and $Co_3O_4$ Nanoparticles: Synthesis, Characterizations, and Raman Spectroscopy

**M. Rashad,[1] M. Rüsing,[2] G. Berth,[2] K. Lischka,[2] and A. Pawlis[2]**

[1] *Physics Department, Faculty of Science, Assiut University, Assiut 71516, Egypt*
[2] *Center of Optoelectronics and Photonics Paderborn (CeOPP), Warburger Straße 100, 33098 Paderborn, Germany*

Correspondence should be addressed to M. Rashad; mohamed.ahmed24@science.au.edu.eg

Received 3 April 2013; Revised 29 June 2013; Accepted 6 July 2013

Academic Editor: Yanbao Zhao



Copper oxide and cobalt oxide (CuO, $Co_3O_4$) nanocrystals (NCs) have been successfully prepared in a short time using microwave irradiation without any postannealing treatment. Both kinds of nanocrystals (NCs) have been prepared using copper nitrate and cobalt nitrate as the starting materials and distilled water as the solvent. The resulted powders of nanocrystals (NCs) were characterized by X-ray diffraction (XRD), transmission electron microscopy (TEM), scanning electron microscopy (SEM), and atomic force microscopy (AFM) measurements. The obtained results confirm the presence of the both of oxides nanopowders produced during chemical precipitation using microwave irradiation. A strong emission under UV excitation is obtained from the prepared CuO and $Co_3O_4$ nanoparticles. The results show that the nanoparticles have high dispersion and narrow size distribution. The line scans of atomic force microscopy (AFM) images of the nanocrystals (NCs) sprayed on GaAs substrates confirm the results of both X-ray diffraction and transmission electron microscopy. Furthermore, vibrational studies have been carried out using Raman spectroscopic technique. Specific Raman peaks have been observed in the CuO and $Co_3O_4$ nanostructures, and the full width at half maximum (FWHM) of the peaks indicates a small particle size of the nanocrystals.

## 1. Introduction

Nanocrystalline semiconductor particles have drawn considerable interest in recent years because of their special properties such as a large surface to volume ratio, increased activity, special electronic properties, and unique optical properties as compared to those of the bulk materials [1, 2]. Moreover, it has been shown that colloidal NCs can be integrated in epitaxial grown layers, which allows for the realisation of real device implementations based on NCs [3]. The oxides of transition metals represent an important class of semiconductors, which have applications in magnetic storage media, solar energy transformation, electronics, and catalysis [4]. Among the oxides of transition metals, copper oxide nanoparticles are of special interest as nanofluids in heat transfer application due to their efficiency. For example it has been reported that 4% addition of CuO improves the thermal conductivity of water by 20% [5]. CuO is a semiconducting compound with a narrow band gap and used for photoconductive and photothermal applications [6]. CuO has attracted much attention because it is the basis of several high-$T_c$ superconductors. CuO is known as p-type semiconductor, which makes it a promising material for gas sensors, magnetic storage media, solar energy transformation, electronics, semiconductors, varistors, and catalysis [7]. The CuO exhibits high activity for photocatalysis of $H_2$ evolution reaction (HER) in oxalic acid solution under simulated sunlight irradiation [8]. $Co_3O_4$ NCs are a promising candidate as anode material for lithium secondary batteries because of its electrochemical capacity and high recharging rate [9]. Hybrid material consisting of $Co_3O_4$ nanocrystals grown on reduced graphene oxide is a high-performance bifunctional catalyst for the oxygen reduction reaction (ORR) and oxygen evolution reaction (OER) [10]. Microwave irradiation has shown very rapid growth in its application to material science due to its unique reaction effects such as rapid volumetric heating and the consequent dramatic increase in reaction rates. Compared with the conventional methods, the microwave synthesis has the advantages of short reaction time, small particle size, narrow particle size

distribution, and high purity [11, 12]. Raman spectroscopy is a powerful nondestructive technique that has been successfully used to study a wide range of materials. Raman spectroscopy is of particular relevance to investigate structural properties of nanosized materials because slight variations are easily detected [13]. Advanced Raman spectroscopy methodologies, such as surface-enhanced Raman spectroscopy (SERS), [14] shell-isolated nanoparticle-enhanced Raman spectroscopy (SHINERS), [15] near-field scanning optical microscopy-Raman (SNOM-Raman) [16], and tip-enhanced Raman spectroscopy (TERS), have been developed for ultrasensitive detection, identification, and dynamic study of molecules (SERS and SHINERS) and material surfaces (TERS) [17, 18].

In this paper we present a new rapid growth method to prepare different monoclinic metal oxide nanocrystals in about 10 min using microwave irradiation without any postannealing treatment. The product has good crystallinity, uniform morphology, and high purity as demonstrated by X-ray diffraction, TEM, and Raman spectroscopy.

## 2. Experimental Technique

A microwave oven with 650 W power (Sanle general electric corp. Nanjing, China) was used. Powder XRD measurements were performed on a Shimadzu XD-3A X-ray diffractometer at the $2\theta$ range from 30 to 60, with monochromatized CuK$\alpha$ radiation ($\lambda = 0.15418$ nm). The scanning electron microscopy (SEM) images pictures were recorded on a JEOL-JEM 200CX scanning electron microscope. The transmission electron microscopy (TEM) images pictures were recorded on a JEOL-JEM 200CX transmission electron microscope, using an accelerating voltage of 80 kV. The samples used for TEM observations were prepared by dispersing some products in ethanol followed by ultrasonic vibration for 30 min, then placing a drop of the dispersion onto a copper grid coated with a layer of amorphous carbon. AFM scans ($10 \times 10\,\mu$m) were performed to measure the morphology of the sample's surface in highly sensitive AFM needle non-contact mode. The samples used for AFM were prepared by dispersing some products in methanol and chloroform (50% to 50%) followed by ultrasonic vibration for 20 min, then sprayed only one drop of the dispersion onto a GaAs substrate. After a short time, the solution of methanol and chloroform is evaporated and only the oxides of CuO or $Co_3O_4$ NCs remain on the GaAs substrate. To measure the absorbance, a solution of methanol and chloroform is used for CuO NCs, while for the $Co_3O_4$ NCs distilled water is used. The absorbance of the NCs in solution was measured in a cuvette with 1 cm diameter. A Shimadzu UV-3100 photospectrometer was used to record the UV-Visible absorption spectra of the as-prepared particles. $\mu$-Raman-spectroscopy was used to study the vibrational properties of the nanoparticle. The Raman spectroscopy was done in a backscattering geometry. For excitation a stabilized DPSS-Laser with 532 nm was used. The spectral analysis was done with a holographic grating and an attached Andor Newton camera with a backlight CCD-chip. A spectral resolution of about 2.3 $cm^{-1}$ was reached. In a typical procedure, 25 mL water solution of 0.2 M $Cu(NO_3)_2{\cdot}6H_2O$ was mixed with 25 mL water solution containing 0.2 M $CO(NH_2)_2$ in a round-bottom flask. The vessel containing the solution was introduced into a microwave oven operating at a maximum power of 800 W for 20 min. The solution boils and undergoes dehydration followed by decomposition with the evolution of large amount of gases. After the solution reaches the point of spontaneous combustion, it begins burning and releases lots of heat, vaporizes all the solution instantly, and becomes a solid powder [19]. A black fine powder of CuO NCs is extracted. After cooling to room temperature, the precipitate was centrifuged and washed with distilled water. The final products were collected for characterizations. The same procedure has been repeated for $Co_3O_4$ NCs using Cobalt nitrate as a starting material.

## 3. Results and Discussion

Figure 1 shows the XRD pattern for CuO and $Co_3O_4$ nanoparticles, respectively. The intensities and angular positions of the peaks are in good agreement with corresponding values [20, 21]. No peaks related to impurity are found in the XRD pattern. In order to understand the phase symmetry of the prepared CuO and $Co_3O_4$ nanocrystals a systematic study on the XRD was performed. Sharp peaks were obtained at angles corresponding to the planes (110), (002), (111), ($\bar{2}$02), and (202). This indicates the monoclinic structure of CuO nanocrystals [22] which was found to be highly crystalline. The XRD pattern obtained from the product (Figure 1(b)) is identical to $Co_3O_4$ NCs. The sharp peaks corresponding to the planes (220), (311), (400), (422), (511), and (440) indicate the monoclinic structure of $Co_3O_4$ nanocrystals which was also found to be highly crystalline. The average size of the both nanocrystals is estimated according to the following Debye-Scherer formula [23]:

$$D = \frac{K\lambda}{\beta \cos\theta}, \tag{1}$$

where the constant $K$ is taken to be 0.94, $\lambda$ is the wavelength of used X-ray used which is CuK$\alpha$ radiation ($\lambda = 1.5406$ Å). $\beta$ is the full width at half maximum of the diffraction peak corresponding to $2\theta$. Using (1), the calculated crystallite sizes are found to be in the range of $14 \pm 1$ nm and $14.5 \pm 1.3$ for CuO and $Co_3O_4$ nanoparticles, respectively.

The size and morphology of the product are analyzed by transmission electron microscopy (TEM). Figures 2(a) and 2(b) show the TEM image of the prepared CuO and $Co_3O_4$ nanoparticles. The TEM image reveals that the product consists of spherical particles with a regular morphology and narrow size distribution. The particle size observed in TEM image is in the range of $10 \pm 2$ nm and $13 \pm 2$ for CuO and $Co_3O_4$ nanoparticles, respectively, which is in good agreement with the calculated results by Scherrer formula (1). The inset Figures 2(a) and 2(b) show that the SEM image of the sprayed CuO and $Co_3O_4$ nanoparticles on GaAs substrate indicates some agglomerated NCs with different sizes due to different concentration. In order to examine the formation of nanoparticles, the surface analysis of sprayed CuO and $Co_3O_4$ nanoparticles on the GaAs substrate was examined

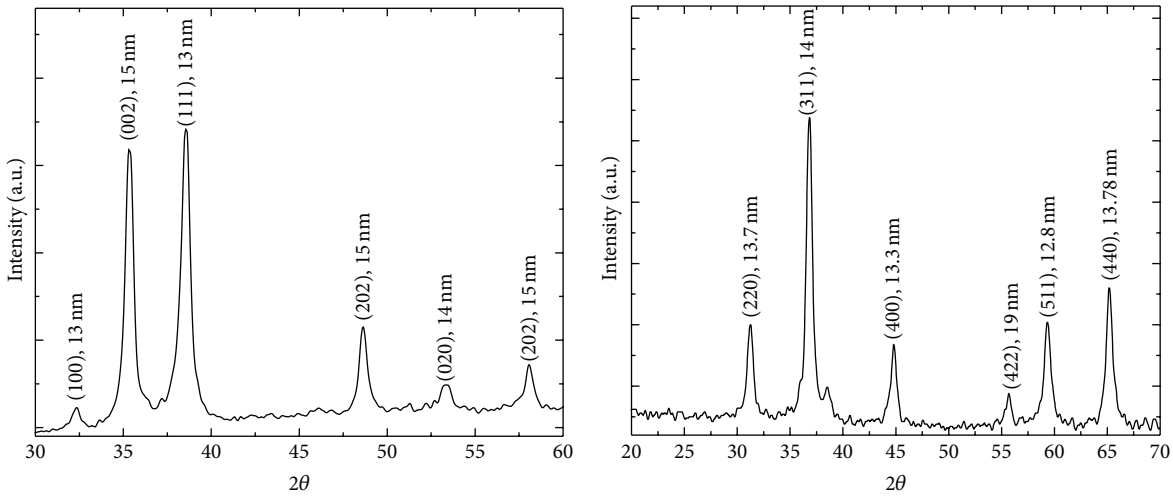


Figure 1: The XRD spectrum of (a) as-prepared CuO and (b) as-prepared $Co_3O_4$ nanoparticles.

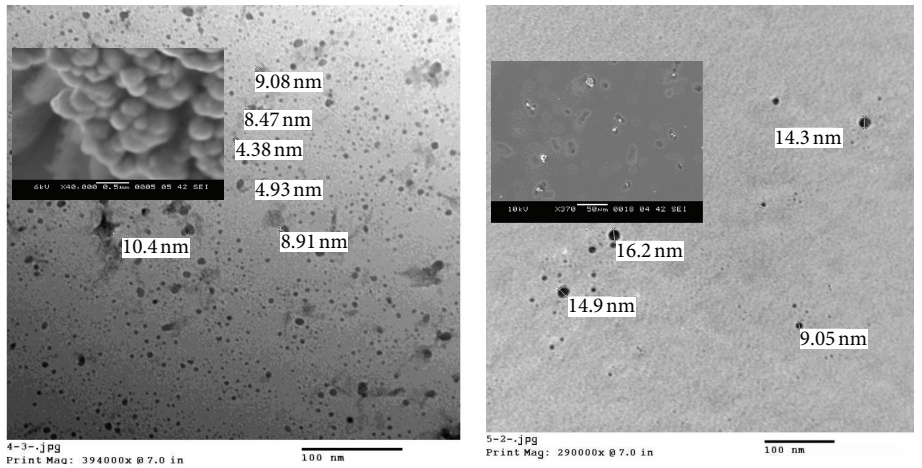


Figure 2: TEM image pattern of (a) as-prepared CuO and (b) as-prepared $Co_3O_4$ nanoparticles.

Table 1: Comparison between the CuO and $Co_3O_4$ nanoparticle sizes calculated from X-ray, TEM, and AFM.

| | X-ray | TEM | AFM |
|---|---|---|---|
| CuO NCs | 14 nm ± 1 | 10 nm ± 2 | 10 nm ± 2 |
| $Co_3O_4$ NCs | 14 nm ± 1.3 | 13 nm ± 2 | 9 nm ± 2 |

Table 2: Positions and FWHM of Raman peaks for as-prepared CuO NCs.

| $A_g$ ($cm^{-1}$) | | $B_g$ ($cm^{-1}$) | | $B_g$ ($cm^{-1}$) | |
|---|---|---|---|---|---|
| Position | FWHM | Position | FWHM | Position | FWHM |
| 282 | 32 | 330 | 35 | 616 | 40 |

by AFM technique. Figures 3(a) and 3(b) show the 2D, 3D, and line scans extracted from AFM image of CuO and $Co_3O_4$ nanoparticles, respectively, sprayed on GaAs substrate. From this image, the height of the particles can be determined. In (Figures 3(a) and 3(b)) single as well as accumulated particles are clearly visible. The height of particles which indicates the particle size is in good agreement with the X-ray and TEM investigations. The calculated size of CuO and $Co_3O_4$ nanoparticles obtained from all characterization techniques are listed in Table 1. Figures 4(a) and 4(b) show the absorbance spectra recorded versus wavelength of CuO and $Co_3O_4$ nanoparticles dispersions in respective solvents. In some cases the measurement of the absorption spectra of prepared CuO NCs yields a small fluctuated band at 270 nm and the other band at 440 nm which is visible in the absorption spectra [12] as illustrated in Figure 4(a). The absorption bands for CuO NCs have been reported to be in the range of 500–600 nm [24–26]. As shown in Figure 4(a), the CuO NCs denote a maximal absorbance at about 490 nm and also a certain contribution in the green and yellow spectral range. This indicates the gradual change of oxidation

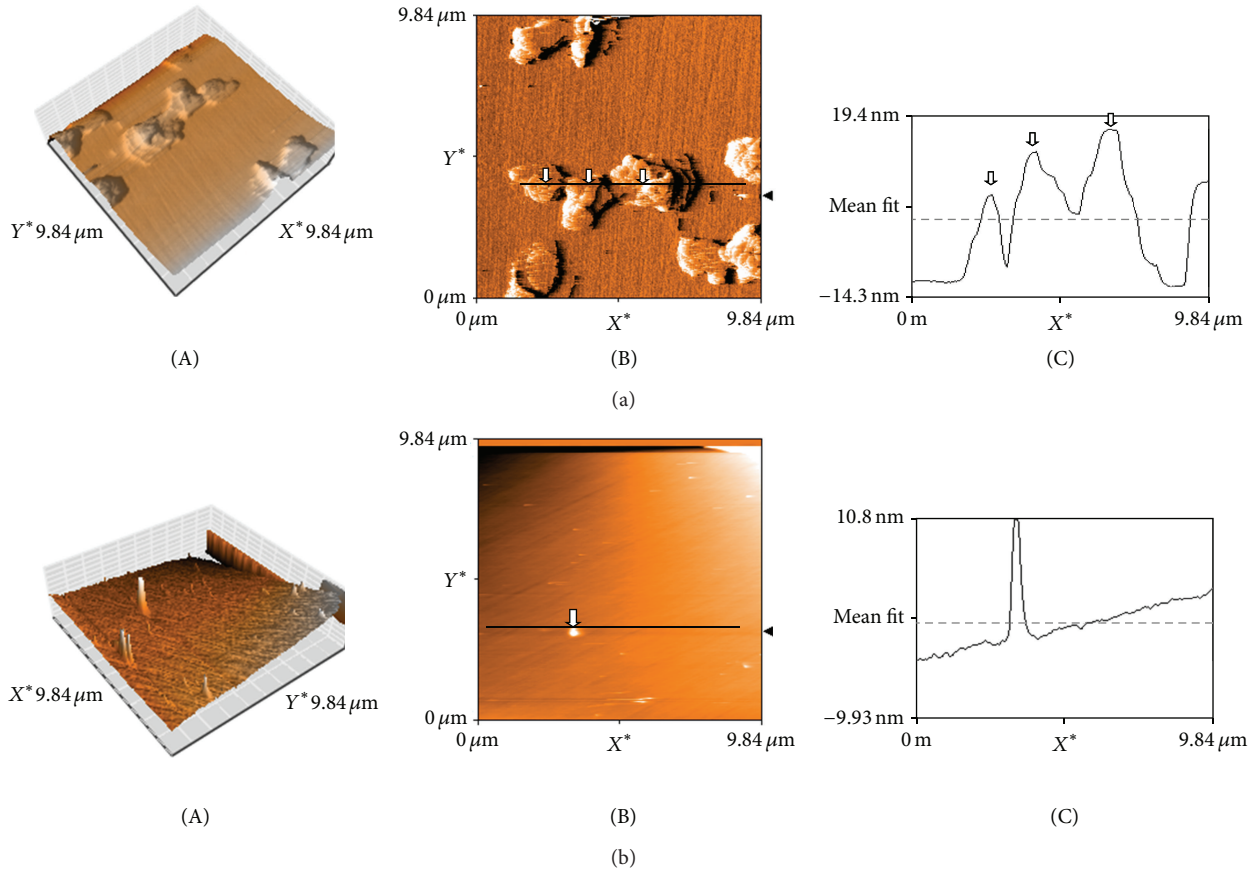


FIGURE 3: (a) AFM image of as prepared CuO nanoparticles (A) 3D, (B) 2D, and (C) line profile of CuO. From (A) and (B), it is confirmed that CuO particles are uniformly distributed on GaAs substrate. In addition, line profile (C) reveals that the size of CuO is around 10 nm. (b) AFM image of as prepared $Co_3O_4$ nanoparticles (A) 3D, (B) 2D and (C) line profile of $Co_3O_4$ NCs. From (A) and (B), it is confirmed that $Co_3O_4$ particles are uniformly distributed on GaAs substrate. In addition, line profile (C) reveals that the size of $Co_3O_4$ is around 9 nm.

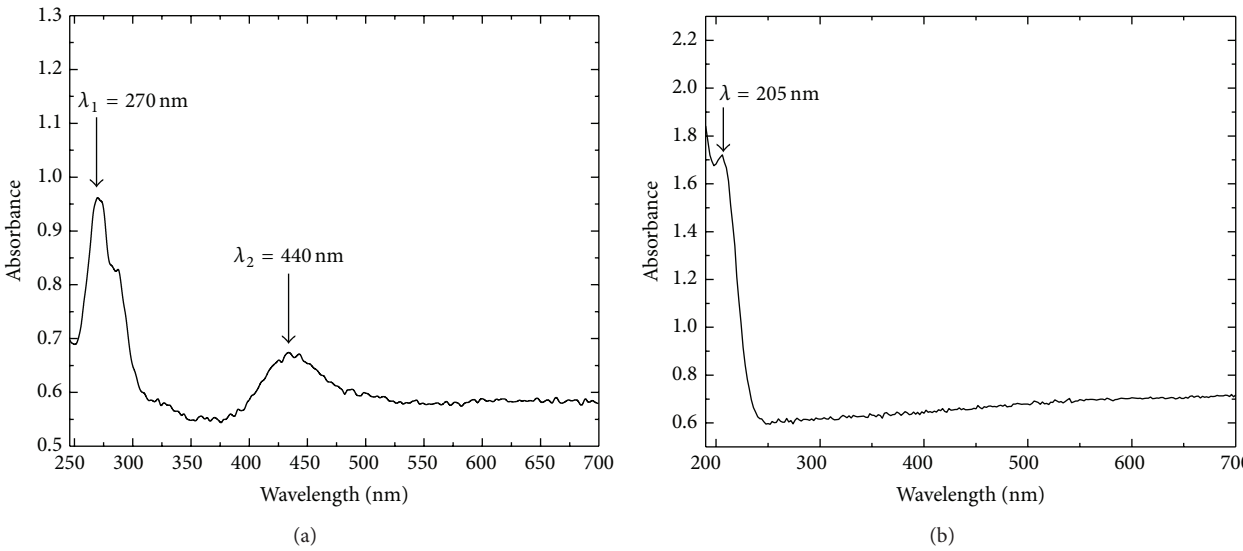


FIGURE 4: (a) Absorbance spectra of as prepared CuO nanoparticles in solution. (b) Absorbance spectra of as prepared $Co_3O_4$ nanoparticles in solution.

Table 3: Positions and FWHM of Raman peaks for as prepared $Co_3O_4$ NCs.

| $F_{2g}$ ($cm^{-1}$) | | $E_g$ ($cm^{-1}$) | | $F_{2g}$ ($cm^{-1}$) | | $F_{2g}$ ($cm^{-1}$) | | $A_{1g}$ ($cm^{-1}$) | |
|---|---|---|---|---|---|---|---|---|---|
| Position | FWHM | Position | FWHM | Position | FWHM | Position | FWHM | Position | FWHM |
| 191 | 10 | 470 | 13 | 510 | 19 | 608 | 12 | 675 | 15 |

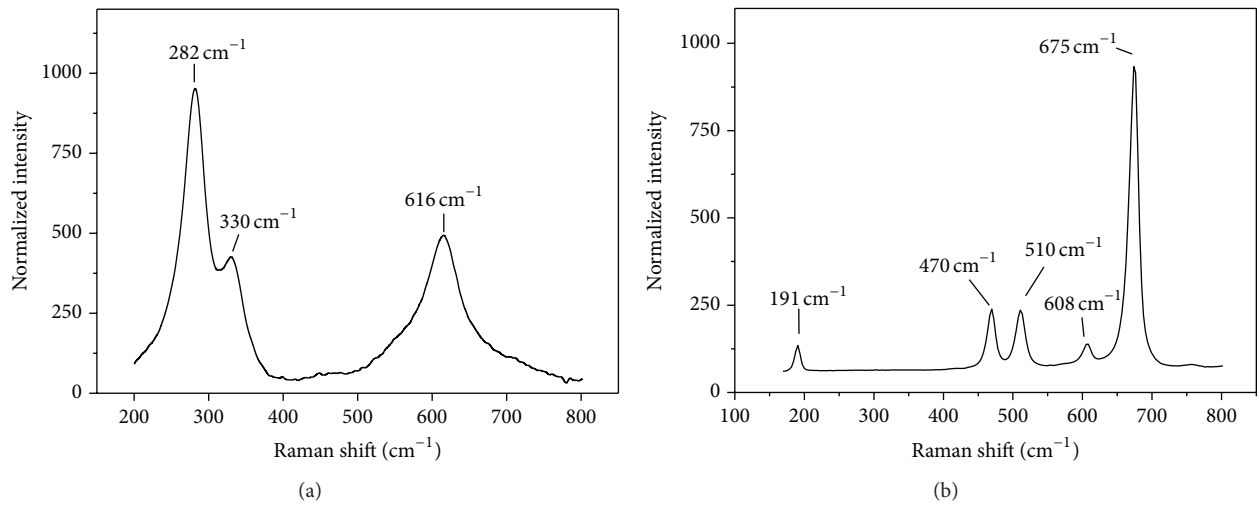


Figure 5: (a) Raman spectra of as prepared CuO nanoparticles. (b) Raman spectra of as prepared $Co_3O_4$ nanoparticles.

state of copper from zero to +2. The peak at 520 nm can be attributed to a narrow size distribution of the particles formed in the solution. Figure 4(b) illustrates the absorbance of $Co_3O_4$ nanoparticles. As can be detected from the figure, the absorption shoulder is centered at 205 nm. This value of the absorption peak position is used to calculate the size of the NCs. A recent result given by [27] shows that the agglomeration state of nanoparticles can produce important modifications on the Raman properties of nanoparticles. An increase of the agglomeration state produces a red-shift and a broadening of the Raman modes similar to those found by nanoparticles size reduction or by temperature increases. Raman spectra of CuO and $Co_3O_4$ nanoparticles are shown in Figure 5. It can be seen from Figure 5(a) that there are three Raman peaks at 282, 330, and 616 $cm^{-1}$. Table 2 lists the experimental results regarding the position and full-width at half maximum (FWHM) of the Raman peaks for as prepared CuO NCs. Our CuO NCs belong to the $C_{2h}^6$ space group with two molecules per primitive cell. There are nine zone-center optical phonon modes with symmetries $4A_u + 5B_u + A_g + 2B_g$; only three $A_g + 2B_g$ modes are Raman active. In comparison with the vibrational spectra of CuO powder [28, 29] and single crystals [30] we can assign the peak at 282 $cm^{-1}$ to the $A_g$ and the peaks at 330 and 616 $cm^{-1}$ to the $B_g$ modes. We note that these wavenumbers are close to those reported in the literature (288, 330 and 621 $cm^{-1}$) [31]. They studied the Raman spectra of CuO nanocrystals with different grain sizes at room temperature and high temperatures up to 873 K. They reported that the intensity is related to the grain size. Stronger and sharper Raman peaks are observed which also shift to longer wavenumbers with increasing/decreasing grain size. Our results are in good agreement with the latter findings. Figure 5(b) shows the Raman spectroscopy of $Co_3O_4$ nanoparticles. Five Raman bands at 191, 470, 510, 608, and 675 $cm^{-1}$ are detected. Table 3 presents the experimental results regarding the position and full-width at half maximum (FWHM) of the Raman peaks for as prepared $Co_3O_4$ NCs. These five Raman active peaks predict the $Co_3O_4$ spinel structure. The Raman mode at 684.5 $cm^{-1}$ ($A_{1g}$) is attributed to characteristics of the octahedral sites and the $E_g$ and $F_{2g}$ modes are likely related to the combined vibrations of tetrahedral site and octahedral oxygen motions [32].

## 4. Conclusion

Nanocrystalline CuO and $Co_3O_4$ particles with a monoclinic structure have been prepared successfully by a novel method using microwave irradiation. The CuO and $Co_3O_4$ NCs are soluble in a chloroform/methanol mixture, thus enabling the processing of these materials in solution. It is a simple and efficient method to produce CuO and $Co_3O_4$ nanocrystals with regular shape, small size, narrow size distribution and high purity. From XRD, SEM, and TEM study, it is found that particles are spherical in shape with average size of 10–14 nm. According to the results of XRD, TEM, and optical properties, we can understand the characteristic features of the investigated metal oxide NCs. Raman scattering performed with CuO and $Co_3O_4$ NCs confirm the NCs formation and estimated size distribution. We can foresee the upscaling of the process to form large quantities of nanosized particles, which have wide applications in various fields such as phonics, catalysis, and biosensors.

## 5. Acknowledgements

This research was supported by the German Research Foundation (DFG), the NTT Basic Research Laboratories, the Commissioned Research of the National Institute of Information and Communications Technology (NICT), the Ministry of Education, Culture, Sports, Science and Technology (MEXT), and the Funding Program for World-leading Innovative Research and Development on Science and Technology (FIRST).

## References

[1] A. Henglein, "Small-particle research: physicochemical properties of extremely small colloidal metal and semiconductor particles," *Chemical Reviews*, vol. 89, no. 8, pp. 1861–1873, 1989.

[2] A. Agfeldt and M. Gratzel, "Light-induced redox reactions in nanocrystalline systems," *Chemical Reviews*, vol. 95, no. 1, pp. 49–68, 1995.

[3] J. Kampmeier, M. Rashad, U. Woggon et al., "Enhanced photoluminescence of colloidal nanocrystals embedded in epitaxially grown semiconductor microstructures," *Physical Review B*, vol. 85, no. 15, Article ID 155405, 2012.

[4] A. S. Lanje, R. S. Ningthoujam, S. J. Sharma, R. B. Pode, and R. K. Vatsa, "Luminescence properties of Sn1-xFex$O_2$ Nanoparticles," *International Journal of Nanotechnology*, vol. 7, no. 9–12, pp. 979–988, 2010.

[5] S. Lee, S. U.-S. Choi, S. Li, and J. A. Eastman, "Measuring thermal conductivity of fluids containing oxide nanoparticles," *Journal of Heat Transfer*, vol. 121, no. 2, pp. 280–288, 1999.

[6] A. E. Rakhshni, "Preparation, characteristics and photovoltaic properties of cuprous oxide, a review," *Solid-State Electronics*, vol. 29, p. 7, 1986.

[7] M. Salavati-Niasari and F. Davar, "Synthesis of copper and copper(I) oxide nanoparticles by thermal decomposition of a new precursor," *Materials Letters*, vol. 63, no. 3-4, pp. 441–443, 2009.

[8] M.-H. Yao, Y.-G. Tang, L. Zhang, H.-H. Yang, and J.-H. Yan, "Photocatalytic activity of CuO towards HER in catalyst from oxalic acid solution under simulated sunlight irradiation," *Transactions of Nonferrous Metals Society of China*, vol. 20, no. 10, pp. 1944–1949, 2010.

[9] P. Poizot, S. Laruelle, S. Grugeon, L. Dupont, and J.-M. Tarascon, "Nano-sized transition-metal oxides as negative-electrode materials for lithium-ion batteries," *Nature*, vol. 407, no. 6803, pp. 496–499, 2000.

[10] Y. Liang, Y. Li, H. Wang et al., "$Co_3O_4$ nanocrystals on graphene as a synergistic catalyst for oxygen reduction reaction," *Nature Materials*, vol. 10, no. 10, pp. 780–786, 2011.

[11] A. G. Saskia, "Microwave chemistry," *Chemical Society Reviews*, vol. 26, no. 3, pp. 233–238, 1997.

[12] H. Wang, J. Xu, J. Zhu, and H. Chen, "Preparation of CuO nanoparticles by microwave irradiation," *Journal of Crystal Growth*, vol. 244, no. 1, pp. 88–94, 2002.

[13] G. Gouadec and P. Colomban, "Raman Spectroscopy of nanomaterials: how spectra relate to disorder, particle size and mechanical properties," *Progress in Crystal Growth and Characterization of Materials*, vol. 53, no. 1, pp. 1–56, 2007.

[14] S. M. Nie and S. R. Emory, "Probing single molecules and single nanoparticles by surface-enhanced Raman scattering," *Science*, vol. 275, no. 5303, pp. 1102–1106, 1997.

[15] J. F. Li, Y. F. Huang, Y. Ding et al., "Shell-isolated nanoparticle-enhanced Raman spectroscopy," *Nature*, vol. 464, no. 7287, pp. 392–395, 2010.

[16] P. G. Gucciardi, S. Trusso, C. Vasi, S. Patanè, and M. Allegrini, "Optical near-field Raman imaging with subdiffraction resolution," *Applied Optics*, vol. 42, no. 15, pp. 2724–2729, 2003.

[17] R. M. Stöckle, Y. D. Suh, V. Deckert, and R. Zenobi, "Nanoscale chemical analysis by tip-enhanced Raman spectroscopy," *Chemical Physics Letters*, vol. 318, no. 1–3, pp. 131–136, 2000.

[18] D. Y. Wu, J. F. Li, B. Ren, and Z. Q. Tian, "Electrochemical surface-enhanced Raman spectroscopy of nanostructures," *Chemical Society Reviews*, vol. 37, no. 5, pp. 1025–1041, 2008.

[19] M. H. Mahmoud, A. M. Elshahawy, S. A. Makhlouf, and H. H. Hamdeh, "Mössbauer and magnetization studies of nickel ferrite nanoparticles synthesized by the microwave-combustion method," *Journal of Magnetism and Magnetic Materials*, vol. 343, pp. 21–26, 2013.

[20] JCPDS cards, No. 5-661.

[21] JCPDS cards, No. 78-1969.

[22] W. T. Yao, S. H. Yu, Y. Zhou et al., "Formation of uniform CuO nanorods by spontaneous aggregation: selective synthesis of CuO, Cu2O, and Cu nanoparticles by a solid-liquid phase arc discharge process," *The Journal of Physical Chemistry B*, vol. 109, no. 29, pp. 14011–14016, 2005.

[23] H. Klug and L. Alexander, *X-Ray Diffraction Procedures*, vol. 125, Wiley, New York, NY, USA, 1962.

[24] J. G. Yang, Y. L. Zhou, T. Okamoto et al., "Preparation of oleic acid-capped copper nanoparticles," *Chemistry Letters*, vol. 35, no. 10, pp. 1190–1191, 2006.

[25] J. G. Yang, T. Okamoto, R. Ichino, T. Bessho, S. Satake, and M. Okido, "A simple way for preparing antioxidation nano-copper powders," *Chemistry Letters*, vol. 35, no. 6, pp. 648–649, 2006.

[26] H. Zhu, C. Zhang, and Y. Yin, "Novel synthesis of copper nanoparticles: influence of the synthesis conditions on the particle size," *Nanotechnology*, vol. 16, no. 12, pp. 3079–3083, 2005.

[27] H. Richter, Z. P. Wang, and L. Ley, "The one phonon Raman spectrum in microcrystalline silicon," *Solid State Communications*, vol. 39, no. 5, pp. 625–629, 1981.

[28] W. Reichardt, F. Gompf, M. Aïn, and B. M. Wanklyn, "Lattice dynamics of cupric oxide," *Zeitschrift für Physik B*, vol. 81, no. 1, pp. 19–24, 1990.

[29] J. Chrzanowske and J. C. Irwin, "Raman scattering from cupric oxide," *Solid State Communications*, vol. 70, no. 1, pp. 11–14, 1989.

[30] H. F. Goldstein, D. Kim, P. Y. Yu, L. C. Bourne, J.-P. Chaminade, and L. Nganga, "Raman study of CuO single crystals," *Physical Review B*, vol. 41, no. 10, pp. 7192–7194, 1990.

[31] J. F. Xu, W. Ji, Z. X. Shen et al., "Raman spectra of CuO nanocrystals," *Journal of Raman Spectroscopy*, vol. 30, no. 5, pp. 413–415, 1999.

[32] C. Woong Na, H. Woo, H. Kim, U. Jeong, J. Hung, and J. Lee, "Controlled transformation of ZnO nanobelts into CoO/$Co_3O_4$ nanowires," *The Royal Society of Chemistry*, 2012.